U.S. Department
of Transportation

**Federal Railroad
Administration**

Evaluation of Elber's Crack Closure Model as an Explanation of Train Load Sequence Effects on Crack Growth Rates

Office of Research and
Development
Washington, DC 20590

Prepared by

D.Y. Jeong
G. C. Sih

Institute of Fracture and Solid Mechanics
Lehigh University
Bethlehem, PA 18015

Prepared for

U.S. Department of Transportation
Research and Special Programs Administration
Transportation Systems Center
Cambridge, MA 02142

DOT/FRA/ORD-90/06

June 1990
Final Report

Technical Report Documentation Page

1. Report No.	2. Government Accession No.	3. Recipient's Catalog No.
DOT/FRA/ORD-90/06	PB90-268624	

4. Title and Subtitle	5. Report Date
Evaluation of Elber's Crack Closure Model as an Explanation of Train Load Sequence Effects on Crack Growth Rates	June 1990
	6. Performing Organization Code: DTS-76
7. Author(s): D.Y. Jeong and G.C. Sih	8. Performing Organization Report No.: DOT-TSC-FRA-90-1
9. Performing Organization Name and Address: Institute of Fracture and Solid Mechanics, Lehigh University, Bethlehem, PA 18015	10. Work Unit No. (TRAIS): RR-019/R-0001
	11. Contract or Grant No.: PR 76-6288
12. Sponsoring Agency Name and Address: U.S. Department of Transportation, Federal Railroad Administration, Office of Research and Development, Washington, DC 20590	13. Type of Report and Period Covered: Final, June 1989 - June 1990
	14. Sponsoring Agency Code: RRS-30

15. Supplementary Notes

16. Abstract

Elber's crack closure model is studied in relation to the results of laboratory spectrum crack growth tests on compact tension specimens (CTS) fabricated from rail steel. Comparison of model predictions with test results for crack growth life is effected by means of an analysis of a center cracked panel (CCP) subjected to an equivalent stress spectrum. (The model cannot be directly applied to the CTS because it is numerically unstable when supplied with finite element approximations for the elastic displacement field at the plastic zone boundary.) The trends of the model predictions and test results agree as to the effect of changing cycle order in the spectrum, but the actual effect on crack growth life in the laboratory tests is found to be much stronger than the effect predicted by Elber's model.

17. Key Words	18. Distribution Statement
Crack Closure, Crack Growth, Spectrum Fatigue Testing, Load Interaction	DOCUMENT IS AVAILABLE TO THE PUBLIC THROUGH THE NATIONAL TECHNICAL INFORMATION SERVICE, SPRINGFIELD, VIRGINIA 22161

19. Security Classif. (of this report)	20. Security Classif. (of this page)	21. No. of Pages	22. Price
Unclassified	Unclassified	29	

Form DOT F 1700.7 (8-72) Reproduction of completed page authorized

PREFACE

The work reported herein was carried out by the Institute of Fracture and Solid Mechanics, Lehigh University. The work is part of an ongoing effort to investigate the effects of alternative descriptions of metal fatigue behavior, in the present case, the fatigue crack propagation behavior of rail steel. The work is sponsored by the Office of Research and Development, Federal Railroad Administration (FRA), and is monitored by the U.S. DOT Transportation Systems Center (TSC), as a part of the FRA/TSC rail integrity research project.

METRIC / ENGLISH CONVERSION FACTORS

ENGLISH TO METRIC

LENGTH (APPROXIMATE)

1 inch (in) = 2.5 centimeters (cm)
1 foot (ft) = 30 centimeters (cm)
1 yard (yd) = 0.9 meter (m)
1 mile (mi) = 1.6 kilometers (km)

AREA (APPROXIMATE)

1 square inch (sq in, in^2) = 6.5 square centimeters (cm^2)
1 square foot (sq ft, ft^2) = 0.09 square meter (m^2)
1 square yard (sq yd, yd^2) = 0.8 square meter (m^2)
1 square mile (sq mi, mi^2) = 2.6 square kilometers (km^2)
1 acre = 0.4 hectares (he) = 4,000 square meters (m^2)

MASS - WEIGHT (APPROXIMATE)

1 ounce (oz) = 28 grams (gr)
1 pound (lb) = .45 kilogram (kg)
1 short ton = 2,000 pounds (lb) = 0.9 tonne (t)

VOLUME (APPROXIMATE)

1 teaspoon (tsp) = 5 milliliters (ml)
1 tablespoon (tbsp) = 15 milliliters (ml)
1 fluid ounce (fl oz) = 30 milliliters (ml)
1 cup (c) = 0.24 liter (l)
1 pint (pt) = 0.47 liter (l)
1 quart (qt) = 0.96 liter (l)
1 gallon (gal) = 3.8 liters (l)
1 cubic foot (cu ft, ft^3) = 0.03 cubic meter (m^3)
1 cubic yard (cu yd, yd^3) = 0.76 cubic meter (m^3)

TEMPERATURE (EXACT)

$[(x - 32)(5/9)]\ ^\circ F = y\ ^\circ C$

ksi	10^3	lb./$in.^2$
ksi $\sqrt{in.}$		

METRIC TO ENGLISH

LENGTH (APPROXIMATE)

1 millimeter (mm) = 0.04 inch (in)
1 centimeter (cm) = 0.4 inch (in)
1 meter (m) = 3.3 feet (ft)
1 meter (m) = 1.1 yards (yd)
1 kilometer (km) = 0.6 mile (mi)

AREA (APPROXIMATE)

1 square centimeter (cm^2) = 0.16 square inch (sq in, in^2)
1 square meter (m^2) = 1.2 square yards (sq yd, yd^2)
1 square kilometer (km^2) = 0.4 square mile (sq mi, mi^2)
1 hectare (he) = 10,000 square meters (m^2) = 2.5 acres

MASS - WEIGHT (APPROXIMATE)

1 gram (gr) = 0.036 ounce (oz)
1 kilogram (kg) = 2.2 pounds (lb)
1 tonne (t) = 1,000 kilograms (kg) = 1.1 short tons

VOLUME (APPROXIMATE)

1 milliliter (ml) = 0.03 fluid ounce (fl oz)
1 liter (l) = 2.1 pints (pt)
1 liter (l) = 1.06 quarts (qt)
1 liter (l) = 0.26 gallon (gal)
1 cubic meter (m^3) = 36 cubic feet (cu ft, ft^3)
1 cubic meter (m^3) = 1.3 cubic yards (cu yd, yd^3)

TEMPERATURE (EXACT)

$[(9/5)y + 32]\ ^\circ C = x\ ^\circ F$

6.895	Megapascals	MPa
1.1	MPa $\sqrt{m}$	

QUICK INCH-CENTIMETER LENGTH CONVERSION

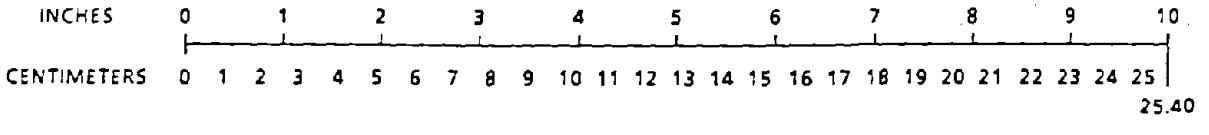

QUICK FAHRENHEIT-CELCIUS TEMPERATURE CONVERSION

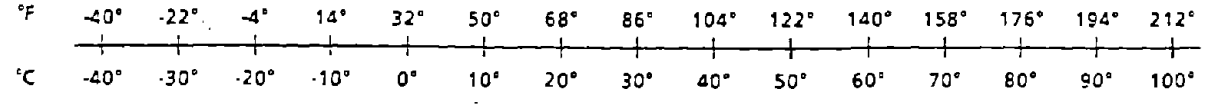

For more exact and/or other conversion factors, see NBS Miscellaneous Publication 286, Units of Weights and Measures. Price $2.50. SD Catalog No. C13 10 286.

TABLE OF CONTENTS

LIST OF FIGURES

LIST OF TABLES

LIST OF ABBREVIATIONS AND SYMBOLS

C - Rate coefficient for crack growth rate equation
c - Crack length
f - Far-field influence function
g - Influence function for plastic zone and wake
K - Stress intensity factor
L - Spring element length
m - Rate exponent for crack growth rate equation
N - Number of spring elements; number of stress cycles
R - Stress ratio
S - Applied stress
W - Plate width
w - Spring element width
x - Spring element location

α - Constraint factor
ΔK - Stress intensity factor range
ΔS - Stress range
ρ - Plastic zone size
σ_0 - Flow stress

EXECUTIVE SUMMARY

This report summarizes the results of a study to assess the applicability of Elber's model to the problem of predicting the fatigue crack growth rates of rail defects. Elber's model, originally proposed in the early 1970s, was the first rational model of load interaction effects in fatigue crack propagation.

Repeated loading of a rail by the wheels of passing trains causes metal fatigue, which often leads to the formation and propagation of a crack in the body of the rail. The wheel loads can "interact" upon a rail fatigue crack, in the sense that the amount by which a particular load makes the crack grow depends on the history of previous loads, as well as the particular load. Evidence for load interaction in rail fatigue exists in the results of field tests of rail crack growth conducted on the Facility for Accelerated Service Testing (FAST) at the Transportation Test Center. Additional evidence has been developed in recent laboratory tests which simulate the rail crack growth environment imposed by the FAST train and by other train makeups representing revenue service.

The rail crack growth models presently in use do not account for load interaction and require empirical correction to achieve agreement with field test results. Also, the laboratory simulation tests suggest that the empirical correction varies with train makeup. Since field test results are not available from revenue track, there is some question whether the present models can provide reliable estimates of crack growth life for rail defects in revenue track, and it is appropriate to consider models which account for load interaction and might thus avoid the need for empirical correction.

The original objective of this study was to precisely match the conditions of two of the laboratory tests. This would have required the application of Elber's model to the laboratory test specimen configuration: a compact tension specimen (CTS) which was designed and dimensioned in accordance with ASTM standards for fatigue crack testing. Since the model requires a description of the specimen deformation pattern under load, the initial approach was to compute approximate deformations from a finite element analysis. However, the model was found to be numerically unstable when supplied with the approximate deformations, and the approach was abandoned.

In order to obtain some quantitative results, Elber's model was applied to a center cracked panel (CCP). The CCP has a much simpler configuration than the CTS and has the advantage of an exact analytical description for its deformation pattern. (The CCP has generally been used in applications of Elber's model to crack propagation analyses in the aerospace industry.)

In order to relate the present analysis to the laboratory results, the test loads were re-converted back to the rail stress specifications from which they had originally been derived. The re-converted stresses were treated as an uniform stress applied to the CCP.

Elber's model was found to be numerically stable when supplied with the analytical CCP deformations. The model predicted trends in crack growth life which were similar to the trends observed in the laboratory tests. However, the test results suggested a much stronger effect of load interaction than the magnitude predicted by the model.

1. BACKGROUND

The research on fatigue crack growth has been long and extensive. However, the mechanics of load sequence effects on crack growth behavior are still not well understood. The cause for acceleration or retardation in the fatigue crack growth behavior has been attributed to a concept known as crack closure. This concept was first hypothesized by Elber [1,2], who conducted fatigue loading experiments on 2219-T851 aluminum alloy specimens. The basic premise was that the crack surfaces are fully open at maximum load, and as the load decreases, the crack surfaces will come into contact at some load greater than the minimum, even if the entire stress cycle is in tension. In the following cycle, the crack remains closed until the load reaches some value above the minimum.

Another way to view the phenomenon is to consider the effects of local plasticity. Residual plastic strains develop in the wake of the advancing crack. The plastic flow in the crack wake is assumed to account for retardation and plasticity ahead of the crack tip is assumed to account for acceleration.

Since Elber's experiments, the study of crack closure has remained largely experimental or phenomenological. Methods for calculating the crack opening stress have addressed constant amplitude loading, for the most part. These methods can be divided into two groups: analytical and those based on finite elements. Newman [3] has used the finite element method to predict the crack opening stress for a center cracked panel. However, the mesh size used to discretize the panel was found to have a strong influence on the results. Newman has also developed an analytical model [4], which was based on a modified Dugdale plastic strip model of the crack-tip plastic zone [5]. Although other analytical models have been developed [6-8], none consider the influence of three

dimensional constraint on the crack closure behavior. In Newman's model, the constraint parameter is assumed and varies depending on whether the problem is assumed to be plane stress or plane strain.

In the study described here, Newman's analytical model was used to predict the crack opening stress and subsequent crack growth for a crack in the center of a finite width plate. Two different stress spectra are considered. These two spectra describe the stress history produced in a rail head by two different trains: the FAST consist and a general freight (GFB) consist. Two different load sequences for each spectrum were also considered: one where the actual load sequence was applied (referred to here as the Real Sequence Order or RSO spectrum) and the other where the order was taken such that the maximum stresses are applied first and the minimum stresses are applied last (refered to here as Decreasing Maximum Stress or DMS spectrum). Jablonski et al. [9] conducted experiments with standard compact tension specimens using these different load spectra. Although an exact comparison between prediction and experiment cannot be made because the test specimens were not center cracked panels, a qualitative comparison may be made.

2. ANALYTICAL MODEL

A brief description of the analytical model to predict the crack opening stress will be given in this section. The analysis can be divided into two parts: (1) the crack opening stress calculation and (2) the crack growth analysis. The model is based on the analytical model of a center crack tension specimen (CCT) developed by Newman [4]. The specimen is assumed to have three distinct regions: (1) a plastic zone ahead of the crack tip; (2) a plastic zone in the wake of the advancing crack; and (3) an elastic continuum

in the remainder of the plate. The actual or physical crack has a dimension of 2c. A fictitious crack of length 2(c+ρ) is assumed in the model where ρ is the length of the plastic zone ahead of each crack tip. The plastic zone is assumed to be loaded by a uniform flow stress. The plastic zone length is calculated based on a modified Dugdale plastic strip model, which assumes small scale yielding. The plastic zone size is the length at constant flow stress such that the stress intensity factor due to the constant flow stress equals the stress intensity factor due to the remotely applied load. In effect, the singularity at the fictitious crack tip is removed. For a finite width CCT panel, the plastic zone ahead of the crack tip at maximum stress, S_{max}, can be calculated from:

$$\rho = c\left\{\frac{W}{\pi c}\arcsin\left[\sin\left(\frac{\pi c}{W}\right)\sec\left(\frac{\pi S_{max}}{2\alpha\sigma_o}\right)\right]-1\right\} \qquad (1)$$

where W is the width of the plate, α is the constraint parameter (which has a value of 1 for plane stress or 3 for plane strain), and σ_o is the flow stress (which is taken to be the average of the ultimate tensile strength and the yield strength).

The four-fold symmetry of the CCT panel allows analysis of half of the crack with one crack tip. The plastic zone ahead of and the wake behind the advancing crack tip are divided into several elements that are assumed to behave as rigid-perfectly plastic springs. The spring element at location x_j is assigned a width of $2w_j$. The element widths become smaller the closer they are to the physical crack tip. Thus, the analysis is performed in a discrete manner.

The length of each of the spring elements in the plastic zone ahead of the crack tip is determined by the crack opening displacement

calculated at the maximum applied stress:

$$L_i = S_{max} f(x_i) - \sum_{j=1}^{N} \alpha\sigma_o g(x_i, x_j) \qquad (2)$$

where $f(x_i)$ and $g(x_i, x_j)$ are influence functions (see Appendix A), and N is the number of spring elements in the plastic zones. These spring element lengths are used as crack opening displacements for a crack that is partially loaded along the crack surfaces and remotely loaded by the minimum applied stress. However, the stresses applied to the crack surfaces (the contact stresses) are unknown and must be found by solving the following system of equations:

$$\sum_{j=1}^{N_{tot}} \sigma_j g(x_i, x_j) = S_{min} f(x_i) - L_i \qquad (3)$$

where N_{tot} is the total number of spring elements used in the model. An iterative solution must be used to find the contact stresses, σ_j, which are bounded by the flow stress. Also, the contact stresses can only take compressive values. The complete set of bounds on element stresses is then as follows:

for elements in the plastic zone ahead of the crack tip ($x_j > c$):

if $\sigma_j > \alpha\sigma_o$ then $\sigma_j = \alpha\sigma_o$
if $\sigma_j < -\sigma_o$ then $\sigma_j = -\sigma_o$

for elements along the crack surfaces ($x_j \leq c$):

if $\sigma_j > 0$ then $\sigma_j = 0$
if $\sigma_j < -\sigma_o$ then $\sigma_j = -\sigma_o$

Note that the constraint parameter α is only applied to tensile stresses, i.e., the stress field is assumed to be uniform through the panel thickness when the crack is closed.

Gauss Seidel iteration appears to be an appropriate algorithm for solving the system of equations (3). An expression for calculating the crack opening stress, S_o, is derived by equating the stress intensity factors due to: (1) a remotely applied load that has a value of the minimum stress minus the crack opening stress; and (2) the contact stresses. For the CCT panel, the crack opening stress can be determined from:

$$S_o = S_{min} - \sum \frac{2\sigma_j}{\pi} [arcsin B_2 - arcsin B_1] \tag{4}$$

where the sum is performed only for the elements along the physical crack surface, and where:

$$B_k = \frac{\sin(\pi b_k / W)}{\sin(\pi c / W)} \quad for \quad k = 1, 2 \tag{5a}$$

$$b_1 = x_j - w_j \tag{5b}$$

$$b_2 = x_j + w_j \tag{5c}$$

The crack growth calculation is performed using a power law formula of the form:

$$\frac{dc}{dN} = C_{eff} (\Delta K_{eff})^m \tag{6}$$

where c is the crack length, C_{eff} is the effective crack growth constant, ΔK_{eff} is the effective stress intensity factor range, and m is the crack growth exponent. For a CCT panel, the effective stress intensity factor range is:

$$\Delta K_{eff} = \Delta S_{eff}\sqrt{\pi c \sec\left(\frac{\pi c}{W}\right)} \tag{7}$$

where ΔS_{eff} is the effective stress range, which depends on the crack opening stress. For constant amplitude loading, the effective stress range is determined by:

$$\Delta S_{eff} = S_{max} - S_o \tag{8}$$

where S_{max} is the maximum applied stress. For variable amplitude loading, the effective stress range, ΔS_{eff}, varies for each cycle and may also depend on the previous load cycle:

if $S_{min_n} < S_{o_n}$ then

$$\Delta S_{eff_n} = S_{max_n} - S_{o_n} \tag{9a}$$

if $S_{min_n} > S_{o_n}$ and $S_{max_n} < S_{max_{n-1}}$ then

$$\Delta S_{eff_n} = S_{max_n} - S_{min_n} \tag{9b}$$

if $S_{min_n} > S_{o_n}$ and $S_{max_n} > S_{max_{n-1}}$ then

$$\Delta S_{eff_n} = \left[(S_{max_n} - S_{o_n})^m - (S_{min_n} - S_{o_n})^m\right]^{1/m} \tag{9c}$$

where S_{min_n}, S_{o_n}, and S_{max_n} are respectively the minimum, opening, and maximum stresses for the n^{th} cycle.

The crack opening stress is calculated for each cycle in a given load spectrum (one block). Thus, the crack growth rate formula is applied on a cycle-by-cycle basis to determine the crack growth increment for one spectrum block. An assumption is now made that the average crack opening stress for that spectrum block will be constant for 0.01 inch of crack growth. That is, the number of blocks required to grow the crack 0.01 inch is calculated based on the cycle-by-cycle analysis for one spectrum block.

3. RESULTS

The results of the analytical model are presented in the form of plots showing crack length as a function of the number of cycles or blocks. The half crack length has an initial length of 0.75 inch. The different load spectra are applied until the crack extends 0.25 inch. The width of the CCT specimen was assumed to be 10 inches.

The following properties for rail steel [10] were assumed in these analyses:

yield strength	72.8 ksi
ultimate strength	135 ksi
modulus of elasticity	30×10^3 ksi
Poission's ratio	0.3

The crack opening stress, however, was found to have weak sensitivity to changes in these material properties.

The effective crack growth constant in eq. (6) is calculated based on an empirical fit of crack growth data from experiments performed on rail steel by Journet [11]:

$$\frac{dc}{dN} = (C_1 R + C_2)\Delta K^m \qquad (10)$$

where $C_1 = 1.537 \times 10^{-10}$, $C_2 = 4.16 \times 10^{-11}$, and m=3.655 are the fitted parameters. The crack growth rates in eqs. (6) and (10) are then equated to define:

$$C_{eff} = (C_1 \overline{R} + C_2)\left[\frac{(1-\overline{R})}{(1-\overline{S_o}/S_{max\,H})}\right]^m \qquad (11)$$

where the bars represent average quantities and $S_{max\,H}$ is the largest maximum stress for a given loading spectrum. The average stress ratios were computed, and the average crack opening stress was calculated from the compliance measurements of crack closure by Jablonski et al. [9]. Thus, an effective crack growth constant was found for each of the four load spectra. The average of the four values for C_{eff} were used in the crack growth calculations. Thus, the parameters used in the crack growth analysis that includes crack closure are:

crack growth rate constant	0.30312×10^{-10}
crack growth exponent	3.655

As shown in Figure 1 and Table 1, the predicted crack growth rate under RSO load sequence is higher than that predicted under DMS for both the FAST and general freight spectra. However, the difference between RSO and DMS is greater for the FAST spectrum than for the general freight. The DMS/RSO life ratios for the two spectra are 1.16 and 1.05, respectively.

Figures 2 and 3 illustrate the histories of calculated crack opening stress for the FAST and general freight spectra,

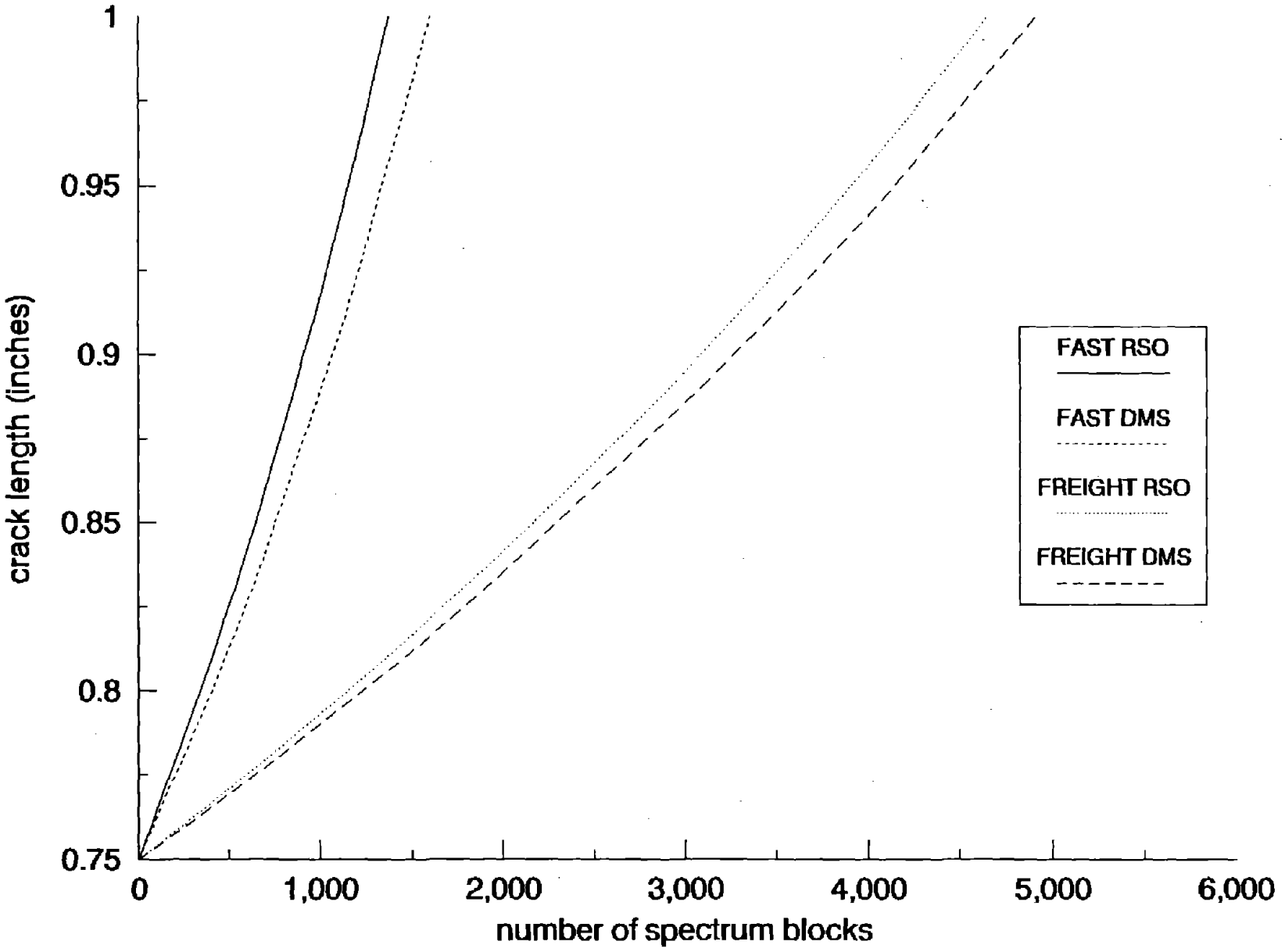

FIGURE 1. LIFE PREDICTIONS BASED ON CRACK CLOSURE MODEL

respectively. In both cases the opening stress is smaller under the RSO spectrum. Changing to DMS order leads increases the opening stress by about 10 percent for the FAST spectrum, and by about 5 percent for the general freight spectrum. The trend of these results generally agrees with the life trends.

TABLE 1. NUMBER OF BLOCKS REQUIRED FOR CRACK GROWTH FROM 0.75 TO 1.0 INCH

Spectrum	Life (blocks)
FAST RSO	1375
FAST DMS	1601
General freight RSO	4651
General freight DMS	4912

Table 2 compares the predicted DMS/RSO life ratios with the results of laboratory tests reported by Jablonksi et al. [9]. The trends are similar, but the difference between RSO and DMS life for the FAST spectrum is much larger in the test results than in the calculations.

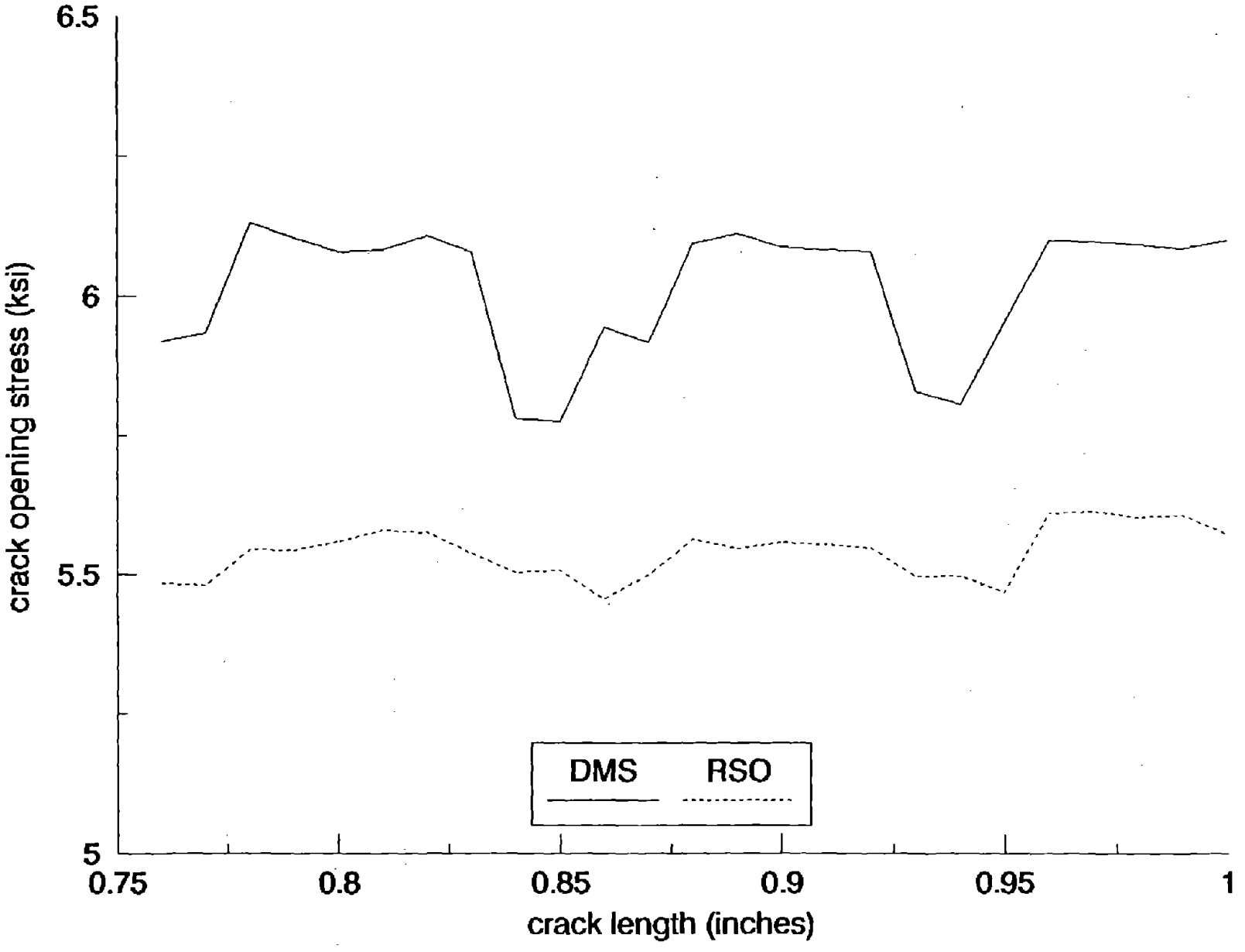

FIGURE 2. CRACK OPENING STRESS HISTORIES PREDICTED FROM FAST SPECTRUM

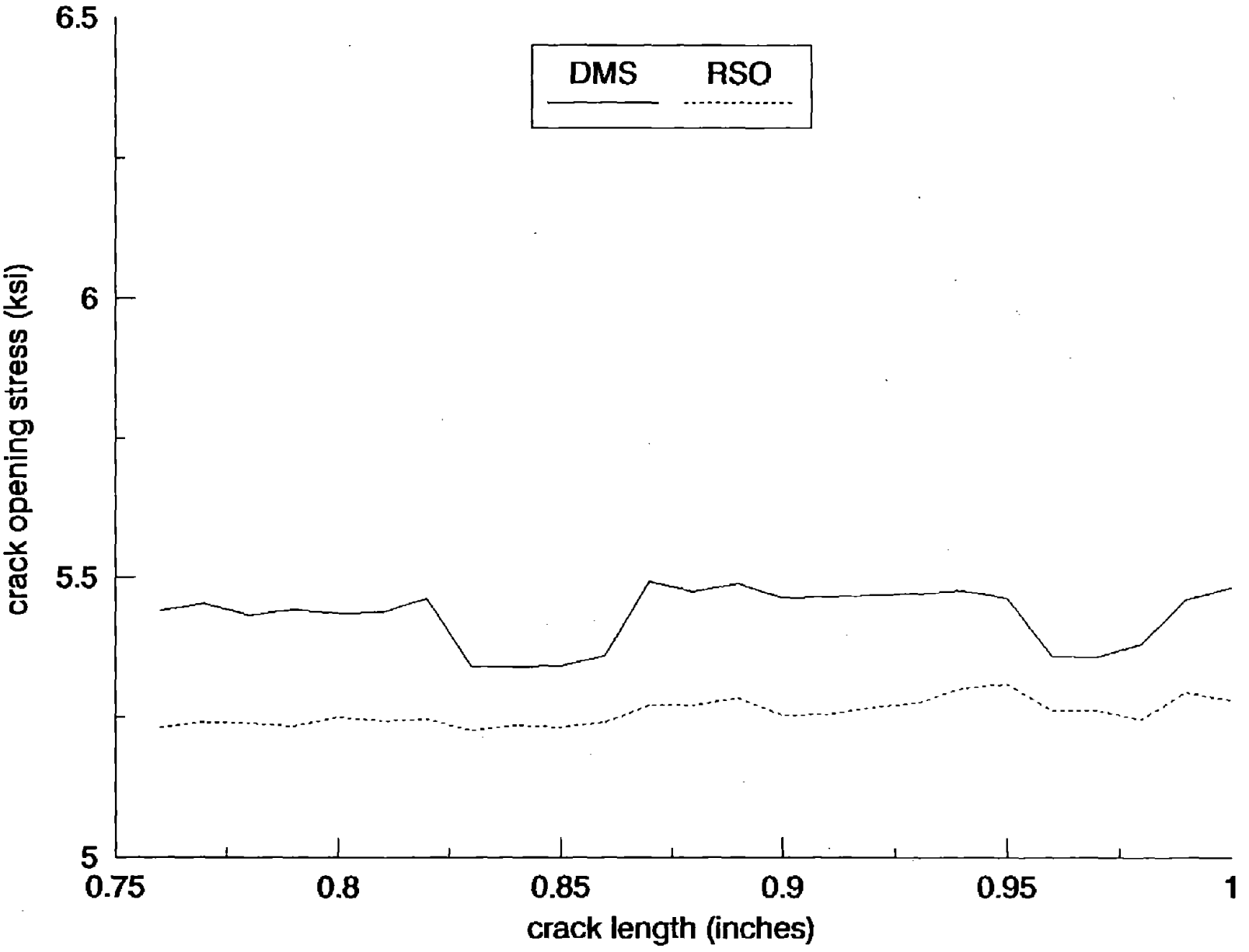

FIGURE 3. CRACK OPENING STRESS HISTORIES PREDICTED FROM GENERAL FREIGHT SPECTRUM

TABLE 2. COMPARISON WITH EXPERIMENTAL RESULTS

Spectrum	DMS/RSO Life Ratio
FAST	
Closure model	1.16
prediction	2.00
Experiment (0.7 - 1.04 in.)	1.95
Experiment (0.7 - 1.39 in.)	
General freight	
Closure model	1.05
prediction	0.87
Experiment (0.7 - 1.04 in.)	1.04
Experiment (0.7 - 1.39 in.)	

4. DISCUSSION AND CONCLUSIONS

The results of the analytical model for crack closure and crack growth appear to be encouraging. The analytical model can be modified for other crack configurations if the solutions for the stress intensity factor and for the crack surface displacements exist under remotely applied loading and for partially loaded cracks.

Unfortunately, closed form solutions do not exist for many crack configurations. At present the only practical applications of the crack closure model appear to be the center cracked panel and, perhaps, the single edge cracked panel, which has some analytical expressions for the stress intensity factors corresponding to remote

loading and to a partially loaded crack. The stress intensity factor for an edge crack of length c in a semi-infinite plane loaded by remote stress, S, is given by [12] as:

$$K = 1.1215S\sqrt{\pi c} \tag{12}$$

Some preliminary calculations have been made for the edge crack geometry. The plastic zone size was found to be larger for the edge crack than for the CCP at the same nominal stress, which was assumed to be one-third the flow stress, and in the case of plane strain (Table 3).

Table 3 - Plastic zone sizes for two crack configurations (in inches)

Constraint condition	CCP (crack length = 2c)	Edge crack (crack length = c)
Plane stress	0.22	0.22
Plane strain	0.021	0.025

The implications of the plastic zone size on the crack opening stress are not known, at this time. However, if the crack opening stress is found to be lower for an edge crack, the fatigue crack will grow faster. Although stress intensity factor solutions exist for a partially loaded edge crack in a semi-infinite medium, the crack surface displacements under the same conditions must also be known in order the determine the influence functions, $f(x_i)$ and $g(x_i, x_j)$.

Although the results presented here are encouraging, the question is still open as to whether crack closure is the sole cause for delay in crack growth behavior [13].

APPENDIX A

INFLUENCE FUNCTIONS FOR CENTER CRACKED PANEL

The influence functions for analyzing the center crack tension specimen are:

$$f(x_i)=\frac{2(1-\nu^2)}{E}\left[(d^2-x_i^2)\sec\left(\frac{\pi d}{W}\right)\right]^{1/2}$$

$$g(x_i,x_j)=G(x_i,x_j)+G(-x_i,x_j)$$

$$G(x_i,x_j)=\frac{2(1-\nu^2)}{\pi E}\{(b_2-x_i)\cosh^{-1}\left(\frac{d^2-b_2x_i}{d\,|b_2-x_i|}\right)-(b_1-x_i)\cosh^{-1}\left(\frac{d^2-b_1x_i}{d\,|b_1-x_i|}\right)$$
$$+\sqrt{d^2-x_i^2}\left[\sin^{-1}\left(\frac{b_2}{d}\right)-\sin^{-1}\left(\frac{b_1}{d}\right)\right]\}\left[\frac{\sin^{-1}B_2-\sin^{-1}B_1}{\sin^{-1}(b_2/d)-\sin^{-1}(b_1/d)}\right]\sqrt{\sec\left(\frac{\pi d}{W}\right)}$$

$$B_k=\frac{\sin(\pi b_k/W)}{\sin(\pi c/W)}\ \text{for k=1,2}$$

where E is the modulus of elasticity, d = c+ρ, $\nu=0$ for plane stress or ν is Poisson's ratio for plane strain, $b_1=x_j-w_j$, and $b_2=x_j+w_j$.

REFERENCES

[1] W. Elber, "Fatigue crack closure under cyclic tension," Engineering Fracture Mechanics 2, pp. 37-45 (1970).

[2] W. Elber, "Significance of fatigue crack closure," Damage Tolerance in Aircraft Structures, ASTM STP 486, pp. 230-242 (1971).

[3] J. C. Newman, "A finite element analysis of fatigue crack closure," Mechanics of Crack Growth, ASTM STP 590, pp. 280-301 (1976).

[4] J. C. Newman, "A crack closure model for predicting fatigue crack growth under aircraft spectrum loading," Methods and Models for Predicting Fatigue Crack Growth Under Random Loading, ASTM STP 748, pp. 53-84 (1981).

[5] D. S. Dugdale, "Yielding of steel plates containing slits," Journal of the Mechanics and Physics of Solids 8, pp. 100-108 (1960).

[6] H. D. Dill and C. R. Saff, "Spectrum crack growth prediction method based on crack surface displacement and contact analyses," Fatigue Crack Growth Under Spectrum Loads, ASTM STP 595, pp. 306-319 (1976).

[7] B. Budiansky and J. W. Hutchinson, "Analysis of closure in fatigue crack growth," Journal of Applied Mechanics 45, pp. 267-276 (1978).

[8] H. Fuhring and T. Seeger, "Dugdale crack closure analysis of fatigue cxcracks under constant amplitude loading," Engineering Fracture Mechanics 11, pp. 99-122 (1979).

[9] D.A. Jablonski, Instron Corporation, Canton, MA, private communication to O. Orringer, DOT Transportation Systems Center, January 23, 1989.

[10] J. J. Scutti, R. M. Pelloux, and R. Fuquen-Moleno, "Fatigue behavior of a rail steel," Fatigue and Fracture of Engineering Materials and Structures 7, pp. 122-135 (1984).

[11] B.G. Journet, "Fatigue crack propagation under complex loading," PhD thesis, Department of Materials Science and Engineering, MIT, 1986.

[12] R. J. Hartranft and G. C. Sih, "Solving edge and surface crack problems by an alternating method," Mechanics of Fracture I: Methods of Analysis and Solutions of Crack Problems, Noordhoff International Publishing (1973).

[13] T. T. Shih and R. P. Wei, "A study of crack closure in fatigue," Engineering Fracture Mechanics 6, pp. 19-32 (1974).